Original Paper

Cellular Physiology and Biochemistry

Cell Physiol Biochem 2012;29:417-430

Accepted: February 10, 2012

S100B Serves as a Ca^{2+} Sensor for ROS-GC1 Guanylate Cyclase in Cones but Not in Rods of the Murine Retina

Xiao-Hong Wen[1†], Teresa Duda[2†], Alexandre Pertzev[2], Venkateswar Venkataraman[3], Clint L. Makino[1] and Rameshwar K. Sharma[2]

[1]Department of Ophthalmology, Massachusetts Eye and Ear Infirmary and Harvard Medical School, Boston, MA, [2]Research Divisions of Biochemistry and Molecular Biology, The Unit of Regulatory and Molecular Biology, Salus University, Elkins Park, PA, [3]Department of Cell Biology, University of Medicine and Dentistry of New Jersey-SOM, Stratford, NJ, [†]Xiao-Hong Wen and Teresa Duda contributed equally to this work

Key Words

Guanylate cyclase • S100B • Phototransduction • Cyclic GMP • Calcium • Retina • Photoreceptors • Knockout mice • Synapse

Abstract

Rod outer segment membrane guanylate cyclase (ROS-GC1) is a bimodal Ca^{2+} signal transduction switch. Lowering $[Ca^{2+}]_i$ from 200 to 20 nM progressively turns it "ON" as does raising $[Ca^{2+}]_i$ from 500 to 5000 nM. The mode operating at lower $[Ca^{2+}]_i$ plays a vital role in phototransduction in both rods and cones. The physiological function of the mode operating at elevated $[Ca^{2+}]_i$ is not known. Through comprehensive studies on mice involving gene deletions, biochemistry, immunohistochemistry, electroretinograms and single cell recordings, the present study demonstrates that the Ca^{2+}-sensor S100B coexists with and is physiologically linked to ROS-GC1 in cones but not in rods. It up-regulates ROS-GC1 activity with a $K_{1/2}$ for Ca^{2+} greater than 500 nM and modulates the transmission of neural signals to cone ON-bipolar cells. Furthermore, a possibility is raised that under pathological conditions where $[Ca^{2+}]_i$ levels rise to and perhaps even enter the micromolar range, the S100B signaling switch will be turned "ON" causing an explosive production of CNG channel opening and further rise in $[Ca^{2+}]_i$ in cone outer segments. The findings define a new cone-specific Ca^{2+}-dependent feature of photoreceptors and expand our understanding of the operational principles of phototransduction machinery.

Introduction

Visual perception involves the transformation of patterns of light and darkness received by the retinal receptors into images of shape defined with depth and color intensity in the visual cortex of the brain. The first stage, termed phototransduction, occurs in the outer segments of the rods and cones (rod outer segment, ROS) where captured photons are converted by a biochemical cascade into electric signals (reviewed in [1, 2]). In darkness, a pair of membrane guanylate cyclases, ROS-GC1 and 2, sustain a basal synthesis of cyclic GMP that

KARGER

Fax +41 61 306 12 34
E-Mail karger@karger.ch
www.karger.com

1015-8987/12/0294-0417$38.00/0

Accessible online at:
www.karger.com/cpb

Xiao-Hong Wen
Department of Ophthalmology, Massachusetts Eye and Ear Infirmary and Harvard Medical School, 243 Charles Street, Boston, MA 02114 (USA)
Tel. +1 617 573-3123, Fax +1 617 573-4290
E-Mail wenx@meei.harvard.edu

keeps open a fraction of cyclic nucleotide gated (CNG) ion channels in the plasma membrane of the rods and cones. A steady influx of Na^+ and Ca^{2+} passes through the open channels and keeps the photoreceptor depolarized. Photons trigger the hydrolysis of cyclic GMP, closing the channels and blocking the entry of cations, thus hyperpolarizing the photoreceptor. Because extrusion of Ca^{2+} by the Na^+/Ca^{2+}-K^+ exchanger persists, there is a light-induced fall in $[Ca^{2+}]_i$ from 250 nM to about 20 nM in mammalian rods [3]. Guanylate cyclase activating proteins (GCAPs) sense the fall in Ca^{2+} and stimulate ROS-GC to synthesize cyclic GMP at a faster rate, limiting the effect of the phototransduction cascade and helping to return the photoreceptor to its resting state (reviewed in [2, 4]).

At the photoreceptor-bipolar cell synapse, in addition to GCAPs, ROS-GC1 activity is regulated by another Ca^{2+} sensor, S100B. Unlike GCAPs, S100B has little effect at low $[Ca^{2+}]_i$ but instead, stimulates ROS-GC1 activity as $[Ca^{2+}]$ approaches micromolar levels [5, 6]. The dual control confers bimodal behavior; ROS-GC1 increases its rate of cyclic GMP synthesis when intracellular $[Ca^{2+}]$ rises to high levels as well as when $[Ca^{2+}]$ falls to very low levels. There is biochemical and immunohistochemical evidence for the presence of S100B in photoreceptor outer segments suggesting some involvement in the phototransduction recovery process [7]. Other studies, however, failed to localize S100B in photoreceptor outer segments, possibly due to species differences [6, 8-11]. Furthermore, S100B has numerous other targets besides ROS-GC1 (reviewed in [12]).

The present study investigates whether ROS-GC1 operates as a bimodal Ca^{2+} transduction switch in the photoreceptor outer segments and explores its underlying biochemical and physiological principles.

Materials and Methods

Genetically Modified Mouse Models

S100B KO mice [13, 14] were generously provided by Dr. Alexander Marks (University of Toronto, ON, Canada) and a colony was maintained at Salus University. Additional mice that were used included: ROS-GC1 KO (GC-E null) mice [15] from Dr. Alexander Dizhoor (Salus University), GCAP1/GCAP2 KO (GCAPs KO) mice [16] from Dr. Alexander Dizhoor with the permission of Dr. Jeannie Chen (University of Southern California). Blocks of processed retinal tissue from Nrl KO mice [17] were kindly provided by Dr. Jerome Roger and Dr. Anand Swaroop (NIH-NEI).

All experiments involving animals were approved by the IACUCs at Salus University and at the Massachusetts Eye and Ear Infirmary and were conducted in strict compliance with the NIH guidelines.

Antibodies

Rabbit S100B and ROS-GC1 antibodies were produced, characterized and affinity purified as in [18, 19]. Other antibodies and serum were obtained from commercial sources: goat S100B (N-15) antibody (Santa Cruz Biotechnology, Santa Cruz, CA), rabbit cone arrestin antibody (Millipore, Temecula, CA), rabbit rhodopsin antibody (Abcam, Cambridge, MA), two secondary antibodies, DyLight 649-conjugated donkey anti-goat and DyLight 448-conjugated donkey anti-rabbit, and normal donkey serum (Jackson ImmunoResearch Laboratories, Inc., West Grove, PA).

Immunohistochemistry

Mice (wild type and genetically modified) were sacrificed by lethal injection of ketamine/xylazine and perfused through the heart, first with a standard Tris-buffered saline (TBS) and then with freshly prepared 4% paraformaldehyde in TBS. Retinas were fixed for 1 h in 4% paraformaldehyde in TBS at 4°C, cryoprotected with 30% sucrose overnight at 4°C, and cut into 20 µm sections. For S100B immunostaining, the sections were washed with TBS, blocked in buffer containing 5% normal donkey serum, 1% BSA in a TBS/0.5% Triton X-100 solution (TTBS) for 1 h at room temperature, washed with a TBS/0.05% Tween-20 solution (TBST), incubated with goat S100B (N-15) antibody (diluted 1:60 in 1% BSA in a TTBS) overnight at 4°C, washed with TBST, incubated with DyLight 649 (excitation, 652 nm; emission, 670 nm)-conjugated donkey anti-goat antibody (diluted 1:200) for 1 h, washed with TBST. For rhodopsin or cone arrestin immunostaining, the sections were incubated with 5% normal donkey serum, 1% BSA in TTBS, washed with TBST, incubated with an appropriate antibody (1:300 dilution for cone arrestin antibody or 1:50 dilution for rhodopsin antibody) for 1 h, washed with TTBS, incubated with a DyLight 488 (excitation, 493 nm; emission, 518 nm)-conjugated donkey anti-rabbit antibody (diluted 1:200) for 1 h, washed with TTBS, and covered with UltraCruz mounting medium. Images were acquired using an inverted Olympus IX81 microscope/FV1000 spectral laser confocal system and analyzed using Olympus FluoView FV10-ASW software. Digital images were processed using Adobe Photoshop (version 7).

Preparation of Outer Segments and Synaptic Membranes of the Outer Retina

Mouse outer segments and outer plexiform layer synaptic membranes were prepared as described previously [20, 21]. Briefly, mouse retinas were dissected out in ice-cold buffer (0.32 M sucrose, 10 mM Tris-HCl, pH 7.4, and 1 mM phenylmethylsulfonyl fluoride; 20 retinas per 10 ml of the buffer) and vortexed for 5 sec. The tubes were then allowed to stand and the supernatant was aspirated to remove ROS. This procedure was repeated three more times. The crude ROS were purified by gradient centrifugation and stored at -150°C. The retinas devoid of outer segments were then hand homogenized with 5 strokes in a Thomas Teflon homogenizer and centrifuged

at 150*g* for 10 min. The supernatant, devoid of cell debris and nuclei, was then centrifuged at 800*g* for 10 min. The pellet, containing the synaptic membranes, was washed twice and stored at -150°C.

Co-Immunoprecipitation

Affinity purified antibodies against ROS-GC1 were coupled to AminoLink® coupling gel (Pierce) according to the manufacturer's protocol. Membranes of the outer plexiform layer from WT mice were isolated in the presence of 1 mM EGTA or 100 μM Ca^{2+} and solubilized in a buffer containing 20 mM Tris-HCl, pH 7.5, 150 mM NaCl, 1% Triton X-100 and 2 mM phenylmethylsulfonyl fluoride. Membranes of the outer plexiform layer from the S100B KO mice were isolated in the presence of 100 μM $CaCl_2$ and solubilized identically as the WT membranes. The solubilized membranes were incubated with AminoLink coupled antibodies overnight at 4°C. The AminoLink-antibody-antigen complexes were spun down and washed several times with the 20 mM Tris-HCl/150 mM NaCl buffer, pH 7.5, containing 1 mM EGTA or 1 mM $CaCl_2$. Bound antigens were eluted using SDS-sample buffer, separated through SDS-polyacrylamide gel electrophoresis and transferred to nitrocellulose membrane. Samples were probed with antibodies against S100B.

Western Blot

After boiling in gel-loading buffer (62.5 mM Tris-HCl, pH 7.5, 2% SDS, 5% glycerol, 1 mM β-mercaptoethanol, 0.005% bromophenol blue), 50 μg of membrane protein were subjected to gel electrophoresis in a buffer containing 25 mM Tris-HCl pH 8.3, 192 mM glycine and 0.1% SDS. Proteins were transferred to Immobilon membranes in the same buffer with the addition of 5% methanol. The blot was incubated in TBST, pH 7.5, with 5% powdered nonfat Carnation milk (blocking buffer) at 4°C. Primary antibodies diluted with the blocking buffer were added and the incubation was continued for 1 h. After rinsing with TBST the blot was incubated with the secondary antibody and then developed using SuperSignal ECL substrate.

Guanylate Cyclase Activity Assay

Membrane fractions (outer segment or outer plexiform layer) prepared from WT, S100B KO, ROS-GC1 KO and GCAPs KO mice were assayed for guanylate cyclase activity. Briefly, membranes were incubated in an assay system containing 10 mM theophylline, 15 mM phosphocreatine, 20 μg creatine kinase and 50 mM Tris-HCl, pH 7.5, in an ice-bath. Free Ca^{2+} was adjusted to the appropriate concentrations with pre-calibrated Ca^{2+}/EGTA solutions (Molecular Probes). Total assay volume was 25 μl. The reaction was initiated by addition of the substrate solution (4 mM $MgCl_2$ and 1 mM GTP, final concentration) and maintained by incubation at 37°C for 10 min. The reaction was terminated by the addition of 225 μl of 50 mM sodium acetate buffer, pH 6.2, followed by heating in a boiling water bath for 3 min. The amount of cyclic GMP formed was determined by radioimmunoassay [22]. For a given experiment, measurements of activity were made at each [Ca^{2+}] three times.

Electroretinogram (ERG)

Eighteen SVE and 129SVE/B6 hybrid WT and 19 S100B KO mice, aged two to four months, were dark-adapted for 8-12 h and then sedated under dim red light with 20 mg/kg ketamine, 8 mg/kg xylazine, and 800 mg/kg urethane, administered as a cocktail. Pupils were dilated with 1% tropicamide/2.5% phenylephrine, applied to the cornea. During the recordings mice were kept on a thermostated warming plate. The corneal electrode consisted of a platinum wire in a small concave transparent plastic holder filled with a drop of water. A 1 msec, unfiltered flash of saturating white light delivered through the window of an aluminum foil-lined ERG recording chamber was used to evoke the maximal a-wave amplitude with 4 min intervals between flashes. Responses were digitized at 4.2 kHz, although in some experiments, the sampling rate was 2.8 kHz. Responses recorded from left and right eyes were generally similar except for four WT mice and two KO mice, in which the b-wave amplitudes of the two eyes differed by more than two-fold. In those six cases, traces from the eye yielding smaller responses were discarded. Oscillatory potentials were isolated as the difference between the recorded trace and a 16.6 Hz digitally filtered version [23], obtained by convolution with a Gaussian (Igor Pro version 5.04B, WaveMetrics, Lake Oswego, OR).

Single Cell Recordings

Photoresponses were recorded from single rods by the suction electrode method [24]. Five WT and five S100B KO mice, aged 10 to 15 weeks, were dark-adapted overnight before an experiment. Dissected retinas were stored in chilled, oxygenated Leibovitz's L-15 medium. A piece of retina was chopped finely, loaded into an experimental chamber, and perfused with enriched Locke's solution equilibrated with 95% O_2/5% CO_2 at 37°C. The Locke's solution contained (mM): 139 Na^+, 3.6 K^+, 2.4 Mg^{2+}, 1.2 Ca^{2+}, 123.3 Cl^-, 20 HCO_3^-, 10 HEPES, 3 succinate, 0.5 L-glutamate, 0.02 EDTA, 10 glucose, and 0.0015 bovine serum albumin (BSA, Fraction V, Sigma), 1% (v/v) minimal essential medium amino acids (Invitrogen), and 1% (v/v) basal medium Eagle vitamins (Sigma). The outer segment of a single rod was pulled into a silanized glass pipette filled with HEPES buffered Locke's, with BSA but lacking bicarbonate (replaced with Cl^-), amino acids and vitamins. Some rods were challenged with high Ca^{2+}: the electrode was filled with a modified Locke's in which Ca^{2+} was raised to 20 mM, 37.6 mM LiCl was added to suppress the exchanger current and NaCl was reduced to 97.4 mM. 0.5 mM IBMX was also added to the pipette solution in some high Ca^{2+} experiments.

Rods were stimulated with light from a xenon source that was passed through an interference filter at 500 nm, neutral density filters and an electronic shutter whose nominal open duration was 3 ms. Responses were recorded with a patch clamp amplifier (Axopatch 200B, Axon Instruments, Union City, CA), low pass filtered at 30 Hz (-3 dB, 8-pole Bessel, Frequency Devices, Haverhill, MA) and digitized at 400 Hz on a MacIntosh computer (Pulse, version 8.31, HEKA Elektronik, Germany). No corrections were made for the delays of ca. 17 ms introduced by low pass filtering. Recorded data were digitally filtered at 12 Hz by convolution with a Gaussian (Igor Pro version 5.04B), which smoothed the waveform without introducing any delay.

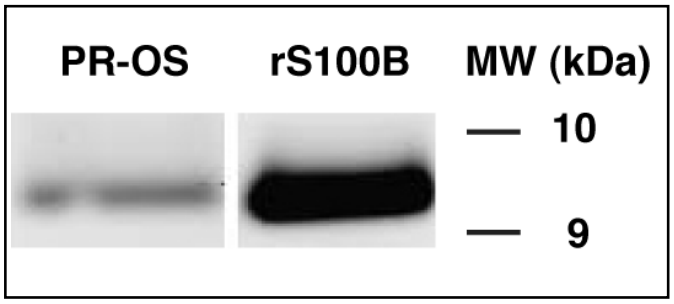

Fig. 1. Expression of S100B in mouse photoreceptor outer segments — Western blot analysis. Proteins from photoreceptor outer segments of WT mice (PR-OS) were solubilized, separated on SDS-16% PAGE, transferred to nitrocellulose, and probed with anti-S100B antibody. The blot was developed using SuperSignal ECL substrate. An immunoreactive band corresponding to S100B appeared at ~ 9 kDa. Bovine S100B expressed in *E. coli* was used as a positive control (rS100B). Molecular weight markers are given on the right.

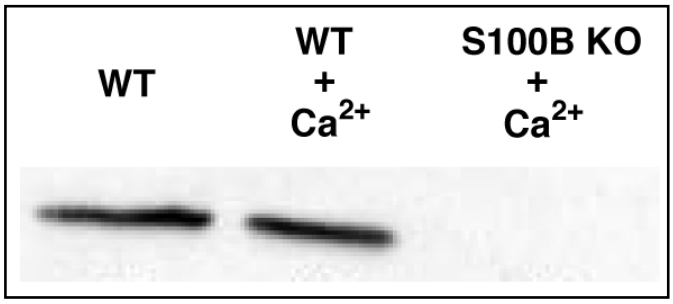

Fig. 2. ROS-GC1–S100B complex in the outer plexiform layer of the mouse retina. Membranes of the photoreceptor-bipolar synaptic layer (OPL) were isolated from WT and S100B KO mouse retinas, solubilized and co-immunoprecipitated with affinity purified ROS-GC1 antibody. The samples were analyzed by Western blotting with anti-S100B antibody. S100B co-immunoprecipitated from WT membranes in the absence of Ca^{2+} (left lane) as well as in its presence (middle lane). S100B was not detected in membranes of S100B KO mice, shown with Ca^{2+} present (right lane).

Results

S100B is expressed in mouse photoreceptor outer segments.

With the overall goal of determining whether S100B is a natural modulator of ROS-GC1 activity linked with phototransduction in retinal photoreceptors, the presence of S100B protein in the photoreceptor outer segments of mice was assessed by Western blotting using affinity purified S100B antibody [18]. An S100B immunoreactive band was present at the expected molecular weight (Fig. 1: lane PR-OS). A band of identical mobility was observed with recombinant S100B (Fig. 1: lane rS100B). Thus, S100B is expressed in mouse photoreceptor outer segments.

Mouse photoreceptor ROS-GC1 is a bimodal Ca^{2+} transduction switch.

To explore the regulation of ROS-GC1 in photoreceptors, it was first ascertained whether the Ca^{2+} bimodal nature of the bovine photoreceptor to bipolar cell synaptic ROS-GC1 system was shared by the mouse photoreceptor-bipolar cell synaptic ROS-GC1 system. The protocol established for isolating bovine photoreceptor-bipolar synaptosomes [19-21] was adapted for the murine retina. Figure 2 shows by co-immunoprecipitation that the ROS-GC1–S100B complex existed in the mouse photoreceptor-bipolar synaptic region and that the complex remained intact under high and low Ca^{2+} conditions. ROS-GC1 was indeed "inhibited" by Ca^{2+} with a $K_{1/2}$ of 124 ± 24 nM and a Hill coefficient of 2.4 ± 0.3

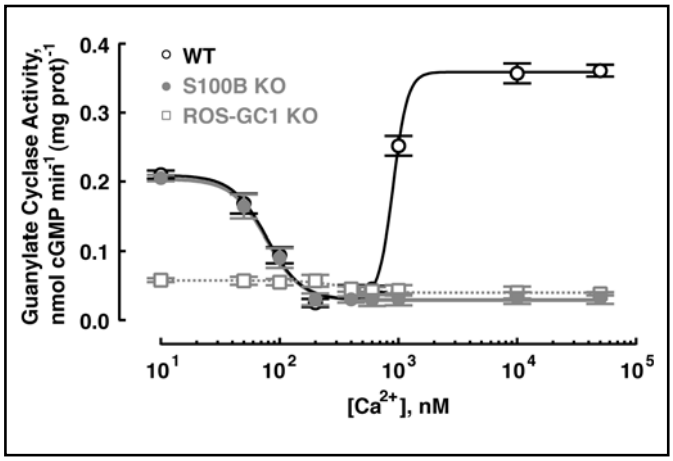

Fig. 3. Ca^{2+} regulation of guanylate cyclase activity in the membranes of the photoreceptor-bipolar synaptic layer of mouse. The OPL membrane fractions, prepared from WT, S100B KO and ROS-GC1 KO mice, were assayed for guanylate cyclase activity as a function of Ca^{2+} concentration. Measurements of each sample were carried out in triplicate and for reproducibility, experiments were repeated three times with separate membrane preparations. The results, shown from one representative experiment, were fit with the Hill function: $K_{1/2}$ = 78 nM, n_H = 3.0 for S100B KO; $K_{1/2}$ = 345 nM, n_H = 6.0 for ROS-GC1 KO. Results from WT membranes were fit with the sum of two Hill functions, where one set of $K_{1/2}$ and n_H were fixed at the values obtained from S100B KO membranes. Upon varying the maximal and minimal activities for each component, the fit returned values of $K_{1/2}$ = 903 nM and n_H = 7.2 for the stimulation of activity at high [Ca^{2+}].

(mean ± SEM, n = 3 experiments) and was stimulated by Ca^{2+} with a $K_{1/2}$ of ~792 ± 55 nM with a Hill coefficient that was not well resolved. These $K_{1/2}$ values match the

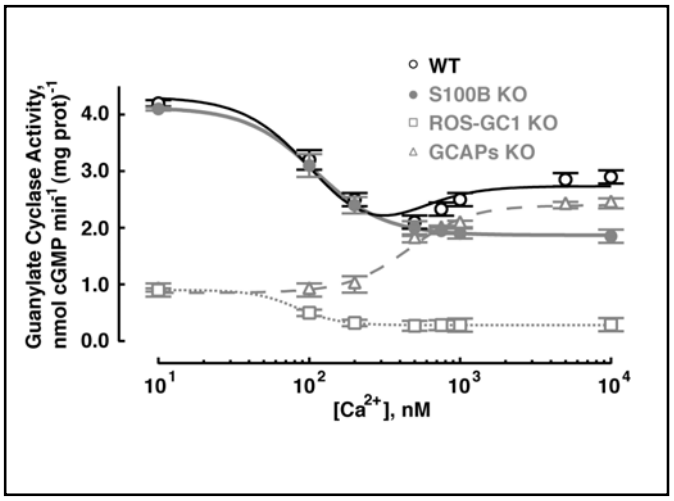

Fig. 4. Ca^{2+} regulation of guanylate cyclase activity in photoreceptor outer segments membranes of WT, S100B KO, ROS-GC1 KO, and GCAPs KO mice. These membranes were assayed for guanylate cyclase activity in the presence of incremental concentrations of Ca^{2+}. Each measurement was made three to six times and experiments with separate membrane preparations were repeated three times. The results shown are from one representative experiment along with fits with the Hill function: $K_{1/2}$ = 109 nM, n_H = 1.9 for S100B KO, $K_{1/2}$ = 82 nM, n_H = 3.1 for ROS-GC1 KO, $K_{1/2}$ = 457 nM, n_H = 2.1 for GCAPs KO. Results from WT membranes were fit with the sum of two Hill functions using $K_{1/2}$ and n_H values determined from S100B KO and GCAPs KO preparations, where maximal and minimal activities for each component were free parameters of the fit.

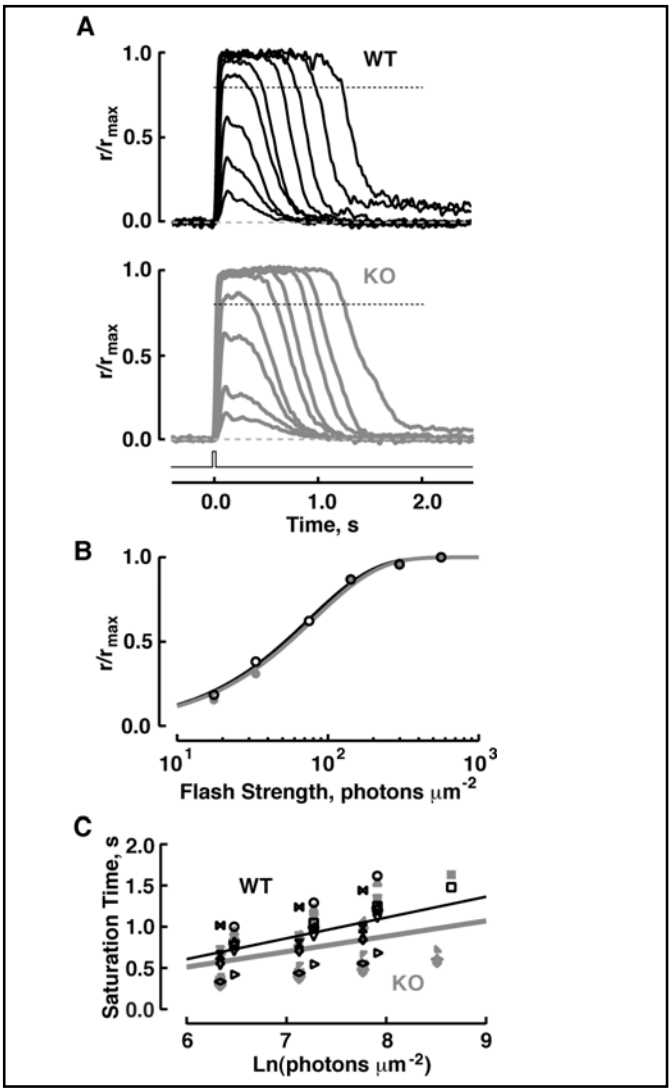

Fig. 5. Identical photoresponses of WT and S100B KO mouse rods. (A) Averaged responses of a WT rod (upper panel) and an S100B KO rod (lower panel) to flashes. Maximal response amplitudes were 8.2 and 7.8 pA for the WT and S100B KO, respectively. Flash strengths were: 18, 33, 75, 142, 298, 564, 1244, 2357 and 4958 photons μm^{-2} for both rods. Flash monitor is shown by the bottom trace. (B) Stimulus-response relations for the rods from A, WT (black symbols) and S100B KO (gray symbols). For illustrative purposes, some saturating responses are not shown. Results were fit with a saturating exponential function, $r/r_{max} = 1- \exp(-ki)$, where i is flash strength, k is equal to $\ln(2)/i_{0.5}$, and $i_{0.5}$ is the flash strength that produces a half-saturating response. $i_{0.5}$ was 54 and 56 photons μm^{-2} for the WT and S100B KO, respectively. (C) Pepperberg plot for WT (black symbols) and S100B KO (gray symbols) rods. The saturation time of a bright flash response was measured from mid-flash to the point at which the saturating response declined to 0.8 r_{max}, i.e., 20% recovery, as demarcated by the dotted lines in A. Values for τ_c, obtained from linear regression (continuous lines), were 252 ms for the 11 WT and 187 ms for 14 S100B KO. The Pearson product moment correlation coefficients for the WT and S100B KO rods were 0.64 and 0.39, respectively.

respective values for bovine photoreceptor-bipolar synaptic membranes of 100 and 800 nM [19]. Only the "inhibitory" phase remained in S100B KO mouse preparations and there was a suggestion that the same held true for ROS-GC1 KO mouse preparations (Fig. 3). Therefore, the mouse photoreceptor-bipolar synaptic ROS-GC1 system was modulated by two sets of Ca^{2+} sensors, GCAPs and S100B, making it a bimodal Ca^{2+} switch.

To address the question whether ROS-GC1 in mouse outer segments also operates as a bimodal Ca^{2+} switch, outer segment membranes of WT mice were analyzed for Ca^{2+}-dependent guanylate cyclase activity (Fig. 4). Guanylate cyclase activity decreased from 4.2 nmol cyclic GMP·min^{-1}·(mg protein)$^{-1}$ at 10 nM [Ca^{2+}] to 2.0 nmol cyclic GMP·min^{-1}·(mg protein)$^{-1}$ at 500 nM [Ca^{2+}]. Then, at higher Ca^{2+} the activity began to rise, reaching 2.7 nmol cyclic GMP·min^{-1}·(mg protein)$^{-1}$ at 10 μM [Ca^{2+}] (n = 3 experiments). The "inhibitory" phase of the guanylate cyclase activity was consistent with the loss of ROS-

	WT	S100B KO	WT, Hi Ca^{2+}	S100B KO, Hi Ca^{2+}
$i_{0.5}$, photons μm^{-2}	42 ± 4, 14	52 ± 4, 15	18 ± 4, 8*	18 ± 4, 4*
Circulating current, pA	8.4 ± 0.4, 15	9.2 ± 0.9, 16	1.6 ± 0.2, 9*	2.3 ± 0.5, 5*
Single photon response amplitude, pA	0.37 ± 0.07, 8	0.37 ± 0.05, 12		
Dim flash response kinetics				
Time to peak, ms	140 ± 4, 9	125 ± 5, 13	211 ± 22, 7*	153 ± 18, 2
Integration time, ms	345 ± 43, 9	326 ± 34, 13	410 ± 62, 7	263 ± 45, 2
Recovery time constant, ms	220 ± 19, 9	246 ± 32, 13	158 ± 48, 7	95 ± 30, 2
τ_c, ms	253 ± 22, 11	226 ± 24, 14	214 ± 17, 6	190 ± 20, 3

Table 1. Photoresponse parameters in WT and S100B KO. Values are given as mean ± SEM, n. Parameters of WT and S100B KO rods did not differ from each other either at normal or elevated $[Ca^{2+}]_i$ based on ANOVA followed by Scheffé tests. For rods of a given type, there were some differences ($p < 0.05$) between values at normal and elevated $[Ca^{2+}]_i$ as indicated by "*". The $i_{0.5}$ is the flash strength at 500 nm that elicits a half-maximal photoresponse, hence it is inversely proportional to sensitivity. Single photon response amplitude was calculated by dividing the ensemble variance by the mean dim flash response amplitude. Single photon response parameters were determined from flash responses whose amplitudes were less than 20% of the maximal response. Time to peak was measured from mid-flash to the response peak. Integration time was calculated as the integral of the response divided by response amplitude. Recovery time constant was obtained from a fit of the final falling phase of the dim flash response with a single exponential. For saturating responses, the slope of linear regression between saturation time and the natural logarithm of the flash strength is referred to as τ_c.

GC1 activation by GCAPs upon Ca^{2+} binding to the latter and the stimulatory phase, on Ca^{2+}-induced activation of ROS-GC1 activity by S100B. These results showed that the mouse photoreceptor outer segment ROS-GC system was indeed a bimodal Ca^{2+} switch.

To confirm this interpretation, outer segment membranes of ROS-GC1 KO, S100B KO, and GCAPs KO mice were analyzed under identical conditions. ROS-GC1 KO fractions showed a marginal Ca^{2+}-dependent "inhibitory" phase and no stimulatory phase (Fig. 4: open squares). The residual guanylate cyclase activity in ROS-GC1 KO was attributed to the relatively low expression of ROS-GC2 activity in rods (~ 10% compared to ROS-GC1) [25, 26]. Modulation by GCAPs supported an "inhibitory" phase but the low affinity of S100B for ROS-GC2 [27] precluded the stimulatory phase. S100B KO mouse fractions had the normal amount of ROS-GC1 and retained "inhibition" by GCAPs with an "IC_{50}" of 108 ± 2 nM Ca^{2+} and Hill coefficient 2.7 ± 0.4 (n = 3) but showed no Ca^{2+}-dependent stimulatory phase (e.g., Fig. 4: closed circles). Finally, GCAPs KO mouse fractions showed only Ca^{2+}-dependent stimulation with $K_{1/2}$ of 510 ± 27 nM and Hill coefficient 2.8 ± 0.5 (e.g., Fig. 4; open triangles). For reasons unknown, the activity of the S100B KO fraction at high $[Ca^{2+}]_i$ did not drop as low as the activity of the GCAPs KO fraction at low $[Ca^{2+}]_i$. The Ca^{2+}-dependence of guanylate cyclase activity of WT outer segment membranes was well described by summing Hill functions obtained for S100B KO membranes and GCAPs KO membranes. Thus S100B modulation of ROS-GC1 supported bimodal switch behavior in mouse outer segments.

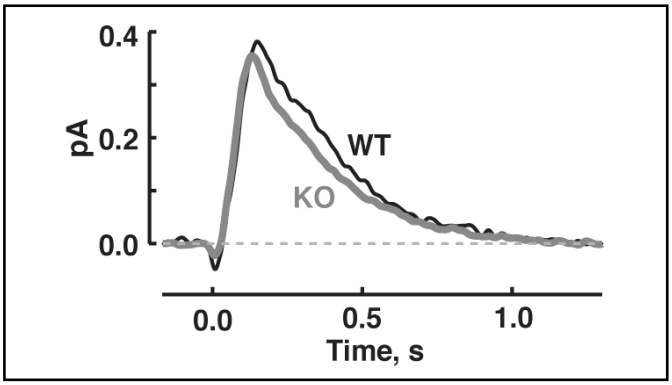

Fig. 6. Similar single photon responses of WT and S100B KO rods. The mean dim flash response, whose amplitude was less than 20% of the maximal response, from each rod was scaled to the amplitude of the single photon response. Then averages were taken for 9 WT rods and 13 S100B KO rods.

S100B does not contribute to rod photoresponses

Flash responses were recorded from WT and S100B KO rods in order to probe for a function of bimodal switching of ROS-GC1 in phototransduction. Had S100B

stimulated ROS-GC1 activity in the dark, the rate of cyclic GMP synthesis in WT rods should have been larger than in S100B KO rods, so there would have been a greater fraction of open CNG channels and a larger circulating current in WT rods. Hence single photon response and maximal response amplitudes should have been lower in S100B KO rods. However, S100B KO rods exhibited normal flash sensitivity, single photon response amplitude and circulating current (Figs. 5, 6 and Table 1). In WT rods, the saturation time of responses to bright flashes increases linearly with the natural logarithm of the flash strength [28, 29]. For S100B KO rods, neither the slope of the relation nor the intercept differed from those of WT (Fig. 5C and Table 1). Also, the single photon response kinetics in S100B KO rods were normal (Fig. 6 and Table 1). These results indicate that under normal physiological conditions, there was no sign that S100B modulated ROS-GC1.

To test the possibility that S100B activity might operate at unnaturally high free Ca^{2+} concentrations, Ca^{2+} inside the pipette was raised 16-fold and LiCl was added. Li^+ resembles Na^+ in carrying current through the CNG channels, but it cripples the Na^+/Ca^{2+}-K^+ exchanger so internal Ca^{2+} could not be removed efficiently [30]. Because high Ca^{2+} concentrations block channel conductance and suppress the circulating current, IBMX was included in some experiments to lower basal PDE activity and open more channels. With 20 mM $CaCl_2$ and 0.5 mM IBMX in the pipette, circulating current increased at first as a small section of rod outer segment was sucked into the pipette, but it soon decreased. Such oscillations recurred as more of the outer segment was drawn into the pipette. The current eventually equilibrated when the entire outer segment was inside the pipette. Even under these conditions the photoresponse of S100B KO rods was indistinguishable from that of WT rods (Fig. 7 and Table 1). Therefore the ROS-GC1–S100B system was not functionally linked to phototransduction in rod outer segments.

S100B is expressed in mouse cone outer segments

To resolve the apparent discrepancy between the biochemical and physiological results, a detailed histochemical analysis of S100B expression in the mouse retina was undertaken. In the WT mouse retina S100B immunoreactivity was clearly observed in some photoreceptor outer segments (Fig. 8A). As observed earlier [6], S100B was also present in the outer plexiform, inner nuclear, and ganglion cell layers. Stained cells included Muller cells, with nuclei in the inner nuclear layer

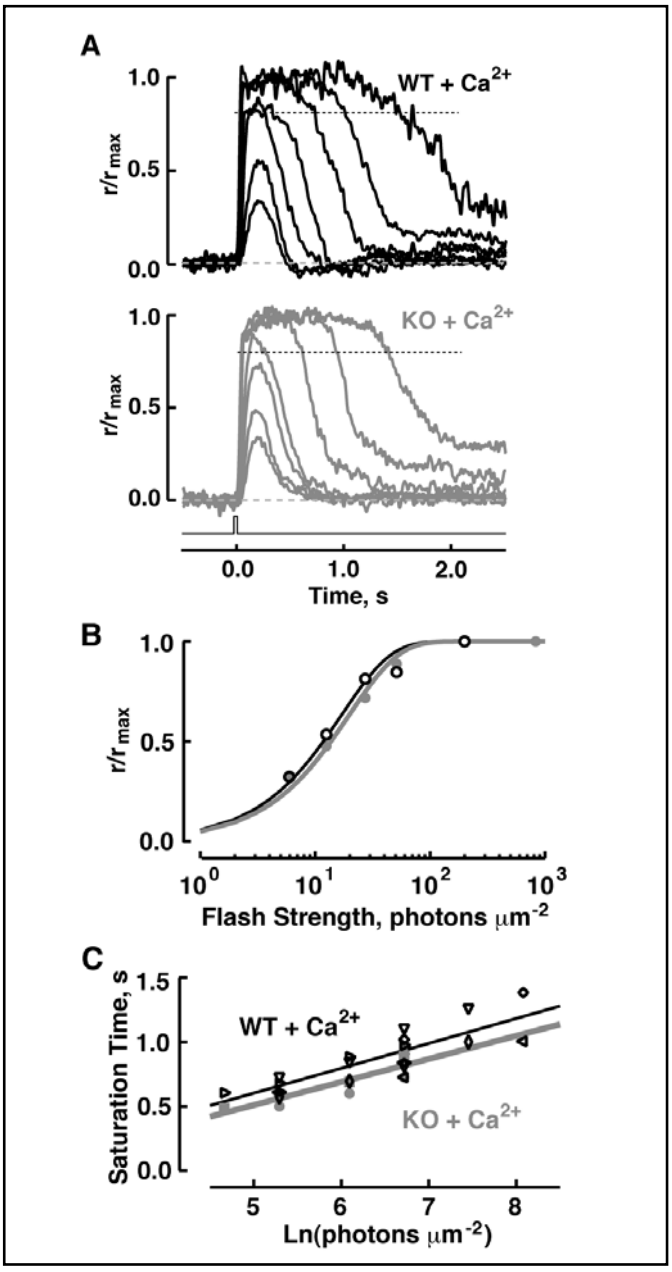

Fig. 7. Indistinguishable photoresponses of WT and S100B KO rods under conditions designed to raise intracellular Ca^{2+}. (A) Averaged responses of the WT rod photoreceptor (upper panel) and a S100B KO rod photoreceptor (lower panel) to flashes of: 6, 13, 27, 51, 199, 827 and 3232 photons μm^{-2} for both rods. Maximal response amplitudes were 2.6 and 3 pA, respectively. Flash monitor is shown as the bottom trace. (B) Stimulus-response relations for the rods from A, WT (black symbols) and S100B KO (gray symbols); some saturated-response points were omitted from each rod for illustrative purposes. $i_{0.5}$ was 12 and 14 photons μm^{-2} for the WT and S100B KO, respectively. (C) Pepperberg plot for WT (black symbols) and S100B KO (gray symbols) rods. Values for τ_c, given from linear regression (continuous lines), were 194 ms for the 6 WT and 180 ms for 3 S100B KO. The Pearson product moment correlation coefficients for the WT and S100B KO rods were 0.84 and 0.88, respectively.

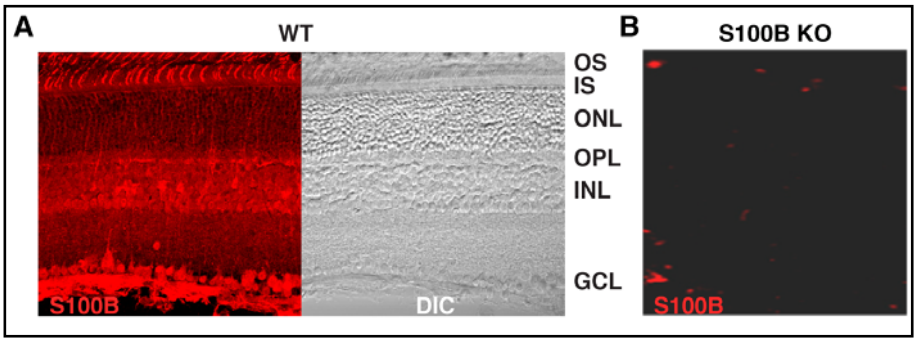

Fig. 8. Immunohistochemical localization of S100B in cryosections from WT (A) and S100B KO (B) mouse retinas. In the cryosections of WT mouse S100B was present in all retinal layers. The staining was absent in S100B KO mouse retina. Differential interference contrast (DIC) image of retinal section showing the retinal layers is shown next to the WT section. The retinal layers are labeled: OS - outer segments; IS - inner segments; ONL - outer nuclear layer consisting of the photoreceptor nuclei; OPL - outer plexiform layer consisting of the synaptic connections of photoreceptors to second order neurons; INL - inner nuclear layer; GCL - ganglion cell layer.

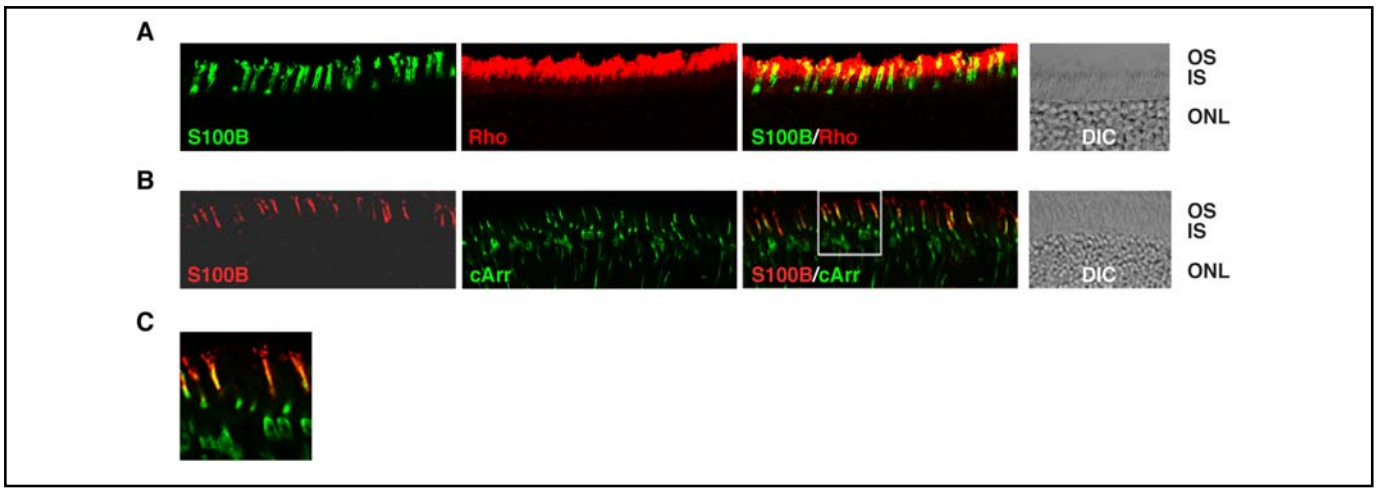

Fig. 9. Expression of S100B in cones. Cryosections from WT mouse retina were doubly immunostained with antibodies against S100B and rhodopsin (A) or S100B and cone arrestin (B). To focus on the photoreceptors, only the photoreceptor and part of the outer nuclear layers are shown. Images labeled "S100B", "Rho" (rhodopsin) and "cArr" (cone arrestin) show immunostaining with the respective antibody only; images labeled "S100B/Rho" and "S100B/cArr" show the composites. The region framed in the "S100B/cArr" image is enlarged as (C). For reference, DIC images show the retinal layers of the sections.

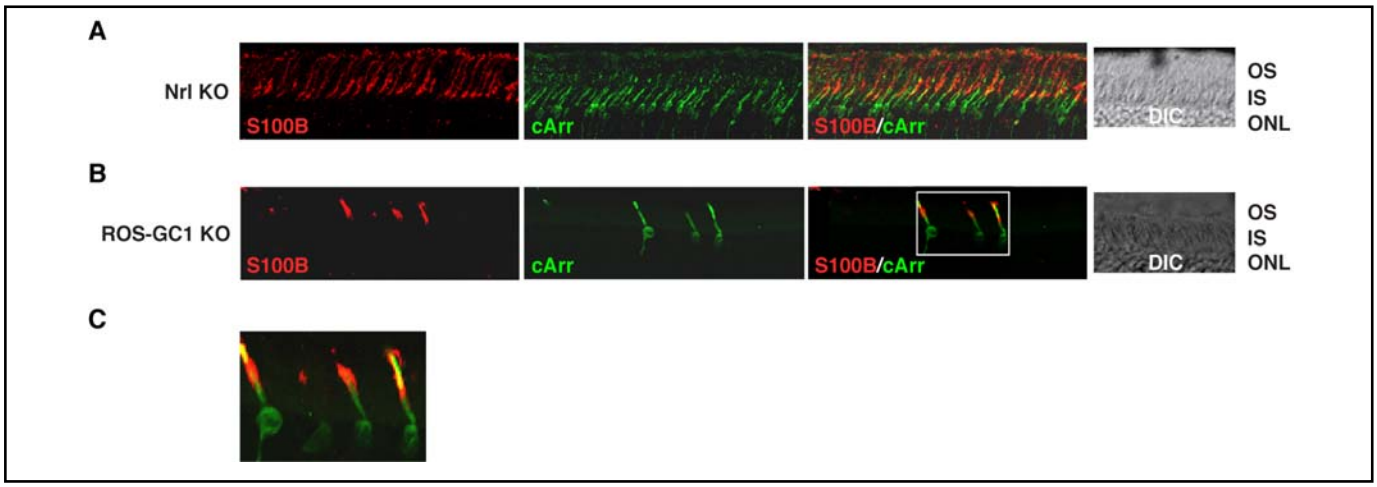

Fig. 10. Immunohistochemical localization of S100B in the retinas of the Nrl KO and ROS-GC1 KO mice. Cryosections from Nrl KO (A) and ROS-GC1 KO (B) mice retinas were stained with antibodies against S100B and cone arrestin. To focus on the photoreceptors, only the photoreceptor and part of the outer nuclear layers are shown. Nrl KO mice do not develop rods in their retinas; all photoreceptors are cones; in the retinas of ROS-GC1 KO mice, cones degenerate. Images labeled "S100B" and "cArr" show immunostaining with only S100B or cone arrestin antibody. Images labeled "S100B/cArr" show co-staining with both antibodies. The region framed in figure (B) "S100B/cArr" is enlarged as (C). DIC images show integrity of the sections.

and radial processes extending from the outer limiting membrane at the top of the outer nuclear layer to the inner limiting membrane just beyond the ganglion cell layer. In contrast, the corresponding layers in the S100B knockout mice retina showed no staining (Fig. 8B). These results confirmed the Western blot results that S100B was expressed in photoreceptor outer segments. The absence of any staining in cryosections of the S100B KO mouse retina attested to the specificity of the S100B antibody; there was no cross-reactivity with S100A1, another member of the S100 family, which is also expressed in photoreceptor outer segments (reviewed in [31]).

The scattered S100B staining of outer segments suggested that it might have been limited to cones. To find out, cryosections of WT mouse retinas were probed either with antibodies against S100B and a rod selective marker, rhodopsin, or with antibodies against S100B and a cone selective marker, cone arrestin. Staining with rhodopsin antibody was intense (Fig. 9A: "Rho") because rods are the predominant photoreceptors in the mouse retina. "Colabeling" with S100B antibody (the yellow signals in Fig. 9A: "S100B/Rho") probably arose as an artifact due to the small size of mouse rods and cones and the limited resolution of immunohistochemistry. However, expression of S100B in a very small population of rods could not be ruled out. Immuno-staining with cone arrestin (Fig. 9B: "cArr"), as expected, was dispersed. Visual comparisons indicated that cells expressing cone arrestin also expressed S100B (Figs. 9B: "S100B/cArr" and 9C). Thus, S100B was present in cone photoreceptors, including their outer segments, but not in rod photoreceptors.

The above results, although in agreement with the single cell recordings, were unexpected. Hence, for verification, immunohistochemical analyses were carried out with retinas of Nrl KO and ROS-GC1 KO mice. Nrl KO retinas contain no rods but are populated exclusively with cone photoreceptors [17], whereas in ROS-GC1 KO retinas, cones degenerate leaving the rods intact [15]. It was reasoned, therefore, that if indeed S100B were expressed exclusively in cones, all photoreceptors present in Nrl KO retinas would be immunostained with S100B antibody but in ROS-GC1 KO retinas, staining would be limited to the few surviving cones. The results of the immunohistochemical analyses are shown in Figure 10. All photoreceptors in the Nrl KO retina were stained with cone arrestin antibody (Fig. 10A: "cArr") confirming their identity as cones and significantly, all were also immunostained with S100B antibody (Fig. 10A: "S100B" and "S100B/cArr"). Few cones remained in 11 month-old ROS-GC1 KO retinas as evidenced by the paucity of cone arrestin-immunopositive profiles, but those that survived were S100B immunopositive (Figs. 10B: "S100B", "S100B/cArr" and 10C). Therefore, among photoreceptors, S100B expression was restricted to cones and in particular, to their synapses and outer segments.

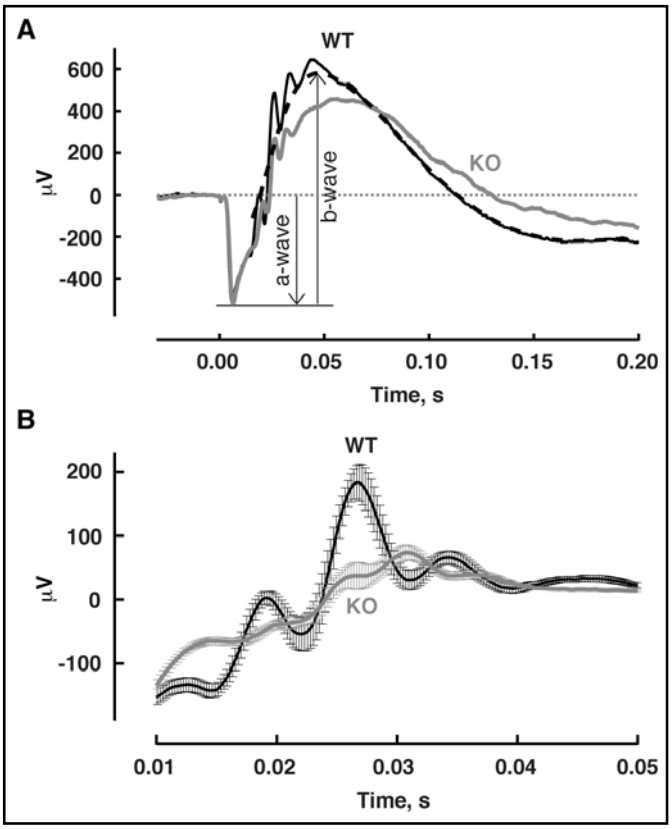

Fig. 11. ERG recordings from WT and S100B KO mice. (A) Representative responses from a WT mouse and an S100B KO mouse to bright flashes that stimulated rods and cones. Traces average 3 trials for WT and 2 trials for S100B KO. Dashed line shows the digitally filtered version of the WT response (see Methods). (B) Smaller oscillatory potentials in S100B KO mice. Oscillatory potentials were extracted from the flash responses of WT and S100B KO as the residuals after digital filtering and then averaged (n = 19 WT mouse eyes and 24 S100B KO mouse eyes). Error bars show SEM.

S100B shapes the retinal response to light

To examine whether S100B contributes to the electrical responses of cone photoreceptors, ERGs were recorded from WT and S100B KO mice (Fig. 11). The ERG is an extracellular field potential that sums the light-

evoked electrical activity of all neurons in the retina, including that of rods and cones (reviewed in [32, 33]). The initial, corneal negative a-wave, generated by the photocurrent responses of the rods, was normal in amplitude in S100B KO mice, consistent with the absence of S100B in WT rods. In S100B KO mice, the corneal positive b-wave, which reflects primarily the amplified responses of rod and cone ON-bipolar cells, peaked at 62 ± 1 msec (n = 19) after the flash, delayed from the time to peak of 49 ± 1 msec (n = 18) for WT mice, $p < 4e\text{-}10$. B-wave was wider in S100B KO. The rise of the b-wave determines the time to peak of the a-wave, which was also slightly delayed in S100B KO mice: 5.7 ± 0.1 msec in WT, 6.3 ± 0.2 msec in S100B KO, $p < 3e\text{-}3$. Although the S100B KO b-wave amplitude was approximately normal, the ratio of the b-wave amplitude to that of the a-wave was reduced from 2.2 in WT to 1.9 in S100B KO (antilogs of the geometric means). A *student's* t-test, performed on $\log_{10}$ (b-wave amplitude/ a-wave amplitude) to minimize distortions in the population distributions caused by the use of ratio transformations, returned $p < 1e\text{-}7$. Oscillatory potentials, arising from activity in the circuitry between bipolar cells, amacrine cells and ganglion cells, superimpose on the rising segment of the b-wave. In comparing the first three peaks of the oscillatory potentials averaged across all mice of each type, those of the S100B KO were smaller in part because the peak-to-peak amplitudes were generally lower in individual S100B KO mice and in part because the timing of the peaks was less consistent across individuals. In addition, each of the peaks arrived on average, about 2 msec later in S100B KO mice. Thus, genetic deletion of S100B shaped the transmission of neural signals, consistent with its presence at the cone synapse and in other cells of the inner retina.

Discussion

The original discovery of the photoreceptor ROS-GC system revealed several unusual signaling features (reviewed in [1, 34, 35]). Contrary to ANF-RGC, the prototype of the membrane bound guanylate cyclase family, ROS-GC1, is not a receptor for natriuretic peptide hormones nor is it regulated by any other extracellular signal. Instead, modulation occurs by changes in $[Ca^{2+}]_i$. Within the outer segments of rods and cones, an increase in $[Ca^{2+}]_i$ from 50 nM to 200 nM cooperatively reduces guanylate cyclase activity [36]. GCAPs were identified as Ca^{2+} sensing subunits responsible for the modulation [37-41]. With Ca^{2+} bound to GCAPs, typical of the resting state in darkness, GCAPs inhibit slightly ROS-GC activity. When $[Ca^{2+}]_i$ falls, e.g. in response to light, Ca^{2+} dissociates from GCAPs, whereupon GCAPs markedly increase ROS-GC activity. This restorative effect on cyclic GMP levels sets the operating range of light intensities under dark and light adapted conditions, accelerates the photoresponse recovery, and suppresses continuous noise due to basal phosphodiesterase activity [16, 42].

Curiously, S100B, purified from a retinal 100,000*g* supernatant fraction also stimulates ROS-GC1 in a Ca^{2+}-dependent fashion, but with $K_{1/2}$ of 1 to 2 μM [5, 6]. While other S100 proteins are capable of substituting for S100B, ROS-GC activity of S100B KO mice was not stimulated at high $[Ca^{2+}]$ in either photoreceptor-bipolar synaptic layer or photoreceptor outer segment membranes (Figs. 3 and 4). For ROS-GC1 to be subject to dual control, it must colocalize with GCAPs and S100B. In the pineal, ROS-GC1 coexists with GCAP1 and S100B but regulation by each Ca^{2+} sensor occurs in separate populations of pinealocytes [43]. At the photoreceptor synapse, ROS-GC1 is coupled to both GCAPs and S100B but the presence of all three components in the same cell is uncertain [6, 19]. Photoreceptor outer segments contain ROS-GC1 and GCAPs but previous studies probing for S100B yielded mixed results [7-11, 44]. Figure 1 shows that S100B is present in outer segments of mouse and Figure 4 demonstrates its modulation of ROS-GC1. Figures 9 and 10 establish that S100B is in cone outer segments and synaptic terminals, while excluding a presence in rods. The requirement for colocalization of ROS-GC1, GCAPs and S100B within cones is thus satisfied. S100B interacts with ROS-GC1 at two sites: Gly^{962}-Asn^{981} and Ile^{1030}-Gln^{1041} [6]. The binding site for GCAP2 is overlapping, but the sites for GCAP1, Met^{445}-Leu^{456} and Leu^{503}-Ile^{522} [45], are distinct, raising the intriguing possibility for simultaneous binding of S100B and GCAP1 to the same ROS-GC1 molecule.

Dual control of ROS-GC1 by GCAPs and S100B creates bimodal Ca^{2+} switching behavior, quickening the rate of cyclic GMP synthesis when $[Ca^{2+}]_i$ falls as well as when it rises above the normal resting levels. GCAPs promote cyclic GMP synthesis at low $[Ca^{2+}]_i$ with a $K_{1/2}$ of ~100 nM whereas S100B acts at high $[Ca^{2+}]_i$ with a $K_{1/2} > 500$ nM (Figs. 3 and 4). The operational dynamics of S100B in the outer segment were not as pronounced as those at the photoreceptor-bipolar synapse (Figs. 3

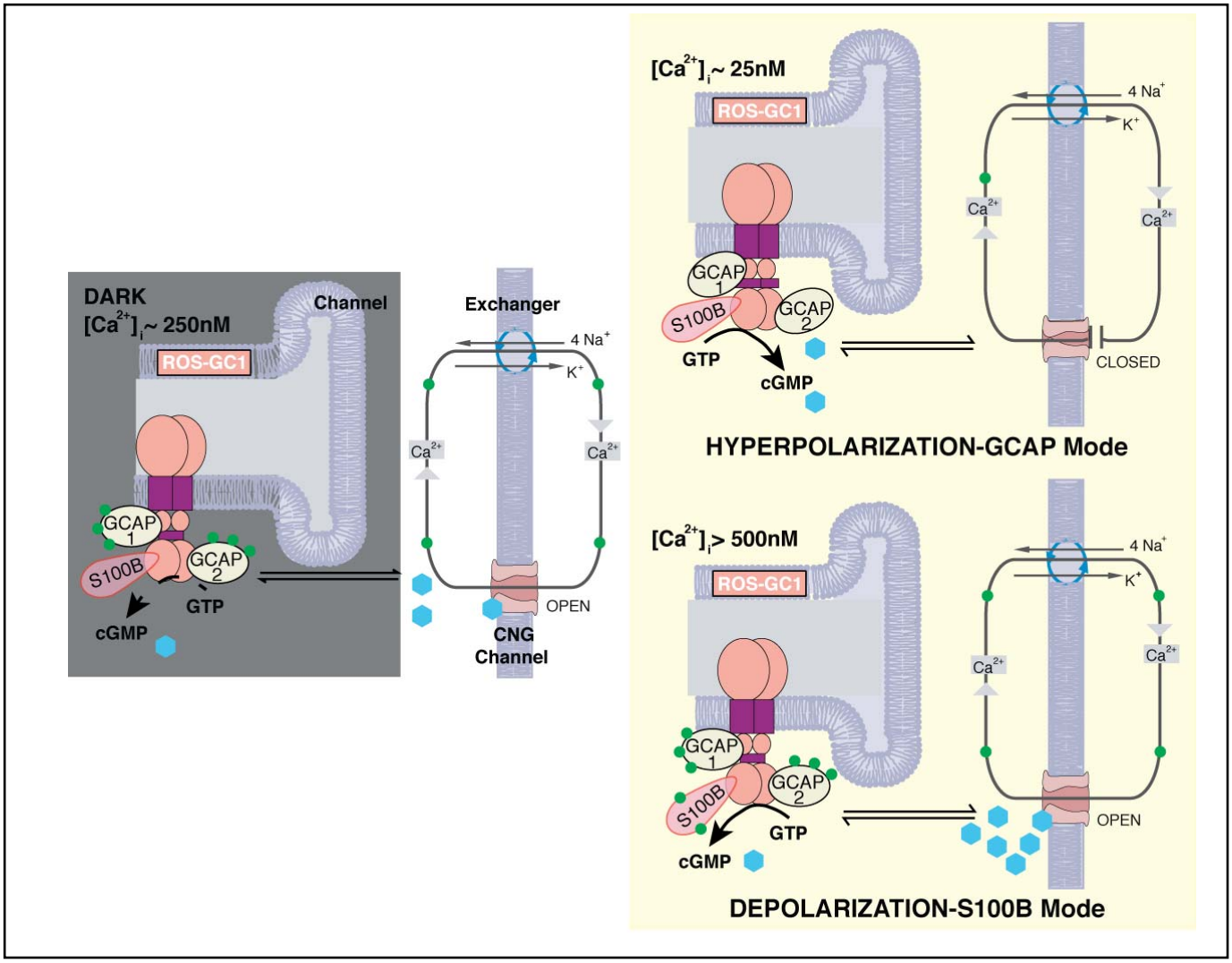

Fig. 12. Two modes of ROS-GC1 modulation by $[Ca^{2+}]_i$ in cones. *Dark state (left).* At $[Ca^{2+}]_i$ = 250 nM Ca^{2+} sensors: GCAP1, GCAP2, S100B are ROS-GC1 bound; GCAP1 and GCAP2 are $[Ca^{2+}]_i$ bound; ROS-GC1 is in the basal state. Cyclic GMP generated keeps a fraction of CNG channels open allowing influx of Na^+ and Ca^{2+}. *Hyperpolarization-GCAP mode (Top right).* LIGHT triggers activation of phosphodiesterase and hydrolysis of cyclic GMP. The decrease in cyclic GMP causes CNG channels to close, preventing influx of Na^+ and Ca^{2+} and hyperpolarizing the outer segment plasma membrane. Extrusion of Ca^{2+} by the Na^+/Ca^{2+}-K^+ exchanger lowers $[Ca^{2+}]_i$ from 250 nM to about 25 nM. The decline causes GCAPs to stimulate ROS-GC1. *Depolarization-S100B mode (Bottom right).* In the pathological state, $[Ca^{2+}]_i$ levels rise above 500 nM. Ca^{2+} is captured by S100B, triggering activation of ROS-GC1. Cyclic GMP formed opens more CNG channels, increasing the influx of Na^+ and Ca^{2+} and raising $[Ca^{2+}]_i$ to even higher levels. Extrusion of Ca^{2+} through Na^+/Ca^{2+}-K^+ exchanger slows as the ion gradients collapse. The cone outer segment membranes stay in ever-DARK-state.

and 4), perhaps reflecting different ratios of GCAPs and S100B at the two cellular domains. Nevertheless, considering that the total ROS-GC activity in outer segment membrane preparations derived mainly from rods while S100B was present only in cones (Figs. 9 and 10), which comprise only a few percent of the total photoreceptor population [46], the nearly 2.5-fold activation of ROS-GC activity in GCAPs KO outer segments at high Ca^{2+} suggested a powerful effect of S100B on ROS-GC1.

Two approaches, ERG and single rod cell recordings, were utilized to determine any physiological linkage of the S100B-modulated ROS-GC1 system with phototransduction. Photocurrent responses recorded from single rods were normal (Figs. 5-7 and Table 1), as was the amplitude of the a-wave component of the ERG, which

summed the photocurrent responses of many rods (Fig. 11). These results support our conclusion that S100B is not expressed in rods. In contrast, the b-wave peaked later in S100B KO mice and recovered more slowly, indicating that S100B modulates the synaptic transmission from cones to ON-bipolar cells. It should be pointed out that while the flash responses of rods were normal in S100B KO mice, no independent measure was available for cones, so the altered bipolar cell response could have involved a disturbance in phototransduction in the cone outer segment. The broader S100B KO b-wave was a sign of increased sensitivity. Yet, the smaller amplitudes of the S100B KO oscillatory potential peaks were more characteristic of decreased sensitivity [47]. The inconsistency means that S100B exerts an influence at more than one site outside the cone outer segment, such as at the cone synapse and in other neurons of the inner retina. Despite the absence of S100B in WT rods, it may still modulate rod signaling. Rod photoresponses affect activity at the cone synapse because mammalian rods and cones are electrically coupled [48-50]. Interestingly, changes in the kinetics of the bipolar cell response without much change in sensitivity could significantly impact overall visual sensitivity, as seen in behavioral tests on recoverin KO mice [51].

In conclusion, co-expression of S100B with ROS-GC1 and GCAPs in cone outer segments and at their synapses confers bimodal Ca^{2+} sensitivity to cyclic GMP synthesis. The operation of the bimodal switch in the outer segment is diagrammed in Figure 12. The GCAPs arm of the switch is essential for the timely recovery of the photoresponse as well as for setting sensitivity and the operating range [42]. Although the physiological significance for the S100B arm is still not well understood, it is predicted that when $[Ca^{2+}]_i$ levels rise under pathological states, for example caused by a Y99C mutation in GCAP1 [52], S100B modulated ROS-GC1 system will be turned "ON". Switching by S100B in intact cells likely occurs at a $[Ca^{2+}]_i$ that is higher than the $K_{1/2}$ of 500 nM observed in our biochemical assays (e.g., Fig. 4), due to the presence of intracellular K^+ [53]. The rise in cyclic GMP might open an excessive number of CNG channels and collapse the ion gradients. In this scenario, S100B might serve a pro-apoptotic role in cones as opposed to the anti-apoptotic role that it plays in other systems (reviewed in [12]). S100B KO cones might then be more resistant to degeneration caused by high Ca^{2+} than wild type cones. While a loss of S100B function appears to be well tolerated in the retina, gain of function mutations may give rise to a retinal dystrophy. Further studies are needed to understand how the presence of S100B at the cone synapse and in other retinal neurons and glia affects visual function and the pathology of retinal disease.

Acknowledgements

We thank Drs. A. M. Dizhoor and A. Savchenko for the ERG recordings. This study was supported by the Lions of Massachusetts, the Pennsylvania Lions Sight Conservation and Eye Research Foundation, the National Eye Institute: EY014104, EY011358, the National Heart Blood and Lung Institute: HL084584 and S82701. The contents herein are the responsibility of the authors and do not necessarily represent the official views of any of the National Institutes of Health.

References

1 Pugh EN, Duda T, Sitaramayya A, Sharma RK: Photoreceptor guanylate cyclases: A review. Biosci Rep 1997;17:429-473.

2 Koch K-W, Duda T, Sharma RK: Ca^{2+}-modulated vision-linked ROS-GC guanylate cyclase transduction machinery. Mol Cell Biochem 2010;334:105-115.

3 Woodruff ML, Sampath AP, Matthews HR, Krasnoperova NV, Lem J, Fain GL: Measurement of cytoplasmic calcium concentration in the rods of wild-type and transducin knock-out mice. J Physiol (Lond) 2002;542:843-854.

4 Detwiler P: Open the loop: Dissecting feedback regulation of a second messenger transduction cascade. Neuron 2002;36:3-4.

5 Pozdnyakov N, Goraczniak R, Margulis A, Duda T, Sharma RK, Yoshida A, Sitaramayya A: Structural and functional characterization of retinal calcium-dependent guanylate cyclase activator protein (CD-GCAP): Identity with S100β protein. Biochemistry 1997;36:14159-14166.

6 Duda T, Koch K-W, Venkataraman V, Lange C, Beyermann M, Sharma RK: Ca^{2+} sensor S100β-modulated sites of membrane guanylate cyclase in the photoreceptor-bipolar synapse. EMBO J 2002;21:2547-2556.

7 Rambotti MG, Giambanco I, Spreca A, Donato R: S100B and S100A1 proteins in bovine retina:Their calcium-dependent stimulation of a membrane-bound guanylate cyclase activity as investigated by ultracytochemistry. Neuroscience 1999;92:1089-1101.

8 Terenghi G, Cocchia D, Michetti F, Diani AR, Peterson T, Cole DF, Bloom SR, Polak JM: Localization of S-100 protein in Müller cells of the retina-1. Light microscopical immunocytochemistry. Invest Ophthalmol Vis Sci 1983;24:976-980.
9 Cocchia D, Polak JM, Terenghi G, Battaglia F, Stolfi V, Gangitano C, Michetti F: Localization of S-100 protein in Müller cells of the retina-2. Electron microscopical immunocytochemistry. Invest Ophthalmol Vis Sci 1983;24:980-984.
10 Molnar ML, Stefansson K, Molnar GK, Tripathi RC, Marton LS: Species variations in distribution of S100 in retina. Demonstration with a monoclonal antibody and a polyclonal antiserum. Invest Ophthalmol Vis Sci 1985;26:283-288.
11 Pozdnyakov N, Yoshida A, Cooper NG, Margulis A, Duda T, Sharma RK, Sitaramayya A: A novel calcium-dependent activator of retinal rod outer segment membrane guanylate cyclase. Biochemistry 1995;34:14279-14283.
12 Donato R, Sorci G, Riuzzi F, Arcuri C, Bianchi R, Brozzi F, Tubaro C, Giambanco I: S100B's double life: Intracellular regulator and extracellular signal. Biochim Biophys Acta 2009;1793:1008-1022.
13 Xiong Z, O'Hanlon D, Becker LE, Roder J, MacDonald JF, Marks A: Enhanced calcium transients in glial cells in neonatal cerebellar cultures derived from S100B null mice. Exp Cell Res 2000;257:281-289.
14 Dyck RH, Bogoch II, Marks A, Melvin NR, Teskey GC: Enhanced epileptogenesis in S100B knockout mice. Brain Res Mol Brain Res 2002;106:22-29.
15 Yang RB, Robinson SW, Xiong WH, Yau KW, Birch DG, Garbers DL: Disruption of a retinal guanylyl cyclase gene leads to cone-specific dystrophy and paradoxical rod behavior. J Neurosci 1999;19:5889-5897.
16 Mendez A, Burns ME, Sokal I, Dizhoor AM, Baehr W, Palczewski K, Baylor DA, Chen J: Role of guanylate cyclase-activating proteins (GCAPs) in setting the flash sensitivity of rod photoreceptors. Proc Natl Acad Sci USA 2001;98:9948-9953.
17 Mears AJ, Kondo M, Swain PK, Takada Y, Bush RA, Saunders TL, Sieving PA, Swaroop A: Nrl is required for rod photoreceptor development. Nat Genet 2001;29:447-452.
18 Duda T, Sharma RK: S100B-modulated Ca^{2+}-dependent ROS-GC1 transduction machinery in the gustatory epithelium: A new mechanism in gustatory transduction. FEBS Lett 2004;577:393-398.
19 Venkataraman V, Duda T, Vardi N, Koch K-W, Sharma RK: Calcium-modulated guanylate cyclase transduction machinery in the photoreceptor–bipolar synaptic region. Biochemistry 2003;42:5640-5648.
20 Redburn DA, Thomas TN: Isolation of synaptosomal fractions from rabbit retina. J Neurosci Methods 1979;1:235-242.
21 Margulis A, Pozdnyakov N, Dang L, Sitaramayya A: Soluble guanylate cyclase and nitric oxide synthase in synaptosomal fractions of bovine retina. Vis Neurosci 1998;15:867-873.
22 Nambi P, Aiyar NV, Sharma RK: Adreno-corticotropin-dependent particulate guanylate cyclase in rat adrenal and adrenocortical carcinoma: Comparison of its properties with soluble guanylate cyclase and its relationship with ACTH-induced steroidogenesis. Arch Biochem Biophys 1982;217:638-646.
23 Lyubarsky AL, Falsini B, Pennesi ME, Valentini P, Pugh EN: UV- and midwave-sensitive cone-driven retinal responses of the mouse: A possible phenotype for coexpression of cone photopigments. J Neurosci 1999;19:442-455.
24 Wen X-H, Shen L, Brush RS, Michaud N, Al-Ubaidi MR, Gurevich VV, Hamm HE, Lem J, Dibenedetto E, Anderson RE, Makino CL: Overexpression of rhodopsin alters the structure and photoresponse of rod photoreceptors. Biophys J 2009;96:939-950.
25 Hwang J-Y, Lange C, Helten A, Höppner-Heitmann D, Duda T, Sharma RK, Koch K-W: Regulatory modes of rod outer segment membrane guanylate cyclase differ in catalytic efficiency and Ca^{2+}-sensitivity. Eur J Biochem 2003;270:3814-3821.
26 Peshenko IV, Olshevskaya EV, Savchenko AB, Karan S, Palczewski K, Baehr W, Dizhoor AM: Enzymatic properties and regulation of the native isozymes of retinal membrane guanylyl cyclase (RetGC) from mouse photoreceptors. Biochemistry 2011;50:5590-5600.
27 Duda T, Goraczniak RM, Pozdnyakov N, Sitaramayya A, Sharma RK: Differential activation of rod outer segment membrane guanylate cyclases, ROS-GC1 and ROS-GC2, by CD-GCAP and identification of the signaling domain. Biochem Biophys Res Commun 1998;242:118-122.
28 Pepperberg DR, Cornwall MC, Kahlert M, Hofmann KP, Jin J, Jones GJ, Ripps H: Light-dependent delay in the falling phase of the retinal rod photoresponse. Vis Neurosci 1992;8:9-18.
29 Nikonov SS, Kholodenko R, Lem J, Pugh EN Jr: Physiological features of the S- and M-cone photoreceptors of wild-type mice from single-cell recordings. J Gen Physiol 2006;127:359-374.
30 Hodgkin AL, McNaughton PA, Nunn BJ: The ionic selectivity and calcium dependence of the light-sensitive pathway in toad rods. J Physiol (Lond) 1985;358:447-468.
31 Rambotti MG, Spreca A, Giambanco I, Sorci G, Donato R: Ultracytochemistry as a tool for the study of the cellular and subcellular localization of membrane-bound guanylate cyclase (GC) activity. Applicability to both receptor-activated and receptor-independent GC activity. Mol Cell Biochem 2002;230:85-96.
32 Peachey NS, Ball SL: Electro-physiological analysis of visual function in mutant mice. Doc Ophthalmol 2003;107:13-36.
33 Weymouth AE, Vingrys AJ: Rodent electroretinography: Methods for extraction and interpretation of rod and cone responses. Prog Retin Eye Res 2008;27:1-44.
34 Sharma RK: Evolution of the membrane guanylate cyclase transduction system. Mol Cell Biochem 2002;230:3-30.
35 Sharma RK: Membrane guanylate cyclase is a beautiful signal transduction machine: Overview. Mol Cell Biochem 2010;334:3-36.
36 Koch KW, Stryer L: Highly cooperative feedback control of retinal rod guanylate cyclase by calcium ions. Nature 1988;334:64-66.
37 Gorczyca WA, Gray-Keller MP, Detwiler PB, Palczewski K: Purification and physiological evaluation of a guanylate cyclase activating protein from retinal rods. Proc Natl Acad Sci USA 1994;91:4014-4018.
38 Dizhoor AM, Olshevskaya EV, Henzel WJ, Wong SC, Stults JT, Ankoudinova I, Hurley JB: Cloning, sequencing, and expression of a 24-kDa Ca^{2+}-binding protein activating photoreceptor guanylyl cyclase. J Biol Chem 1995;270:25200-25206.
39 Frins S, Bönigk W, Müller F, Kellner R, Koch KW: Functional characterization of a guanylyl cyclase-activating protein from vertebrate rods. Cloning, heterologous expression, and localization. J Biol Chem 1996;271:8022-8027.
40 Duda T, Goraczniak R, Surgucheva I, Rudnicka-Nawrot M, Gorczyca WA, Palczewski K, Sitaramayya A, Baehr W, Sharma RK: Calcium modulation of bovine photoreceptor guanylate cyclase. Biochemistry 1996;35:8478-8482.
41 Haeseleer F, Sokal I, Li N, Pettenati M, Rao N, Bronson D, Wechter R, Baehr W, Palczewski K: Molecular characterization of a third member of the guanylyl cyclase-activating protein subfamily. J Biol Chem 1999;274:6526-6535.
42 Sakurai K, Chen J, Kefalov VJ: Role of guanylyl cyclase modulation in mouse cone phototransduction. J Neurosci 2011;31:7991-8000.

43 Venkataraman V, Nagele R, Duda T, Sharma RK: Rod outer segment membrane guanylate cyclase type 1-linked stimulatory and inhibitory calcium signaling systems in the pineal gland: Biochemical, molecular, and immunohistochemical evidence. Biochemistry 2000;39:6042-6052.
44 Kondo H, Takahashi H, Takahashi Y: Immunohistochemical study of S-100 protein in the postnatal development of Müller cells and astrocytes in the rat retina. Cell Tissue Res 1984;238:503-508.
45 Lange C, Duda T, Beyermann M, Sharma RK, Koch KW: Regions in vertebrate photoreceptor guanylyl cyclase ROS-GC1 involved in Ca^{2+}-dependent regulation by guanylyl cyclase-activating protein GCAP-1. FEBS Lett 1999;460:27-31.
46 Carter-Dawson LD, LaVail MM: Rods and cones in the mouse retina. I. Structural analysis using light and electron microscopy. J Comp Neurol 1979;188:245-262.
47 Lachapelle P: Evidence for an intensity-coding oscillatory potential in the human electroretinogram. Vision Res 1991;31:767-774.
48 Raviola E, Gilula NB: Gap junctions between photoreceptor cells in the vertebrate retina. Proc Natl Acad Sci USA 1973;70:1677-1681.
49 Nelson R: Cat cones have rod input: A comparison of the response properties of cones and horizontal cell bodies in the retina of the cat. J Comp Neurol 1977;172:109-135.
50 Schneeweis DM, Schnapf JL: Photovoltage of rods and cones in the macaque retina. Science 1995;268:1053-1056.
51 Sampath AP, Strissel KJ, Elias R, Arshavsky VY, McGinnis JF, Chen J, Kawamura S, Rieke F, Hurley JB: Recoverin improves rod-mediated vision by enhancing signal transmission in the mouse retina. Neuron 2005;46:413-420.
52 Olshevskaya EV, Calvert PD, Woodruff ML, Peshenko IV, Savchenko AB, Makino CL, Ho Y-S, Fain GL, Dizhoor AM: The Y99C mutation in guanylyl cyclase-activating protein 1 increases intracellular Ca^{2+} and causes photoreceptor degeneration in transgenic mice. J Neurosci 2004;24:6078-6085.
53 Baudier J, Glasser N, Gerard D: Ions binding to S100 proteins. I. Calcium- and zinc-binding properties of bovine brain S100 $\alpha\alpha$, S100a ($\alpha\beta$), and S100b ($\beta\beta$) protein: Zn^{2+} regulates Ca^{2+} binding on S100b protein. J Biol Chem 1986;261:8192-8203.